



Comparisons of Sub-Diurnal Wind Vector Variability Near Convection from Models and the Constellation of Scatterometers and Radiometers

F. Joseph (Joe) Turk and Svetla Hristova-Veleva
JPL/Caltech, Pasadena CA

With acknowledgements to Sarah Gille, Thomas Kilpatrick, and Donata Giglio for ideas discussed at the fall 2017 Diurnal Winds Workshop

Remote Sensing Systems, Inc. for providing the extensive radiometer winds datasets

and NASA Ocean Vector Winds ST support

Ocean Vector Winds ST Meeting 24-26 April 2018, Barcelona

2018 California Institute of Technology. U.S. government sponsorship acknowledged.



Science Rationale

A number of studies have focused on the 2003 QuikScat + SeaWinds period (tandem period) to examine diurnal winds (diurnal= first harmonic of the daily cycle).

Findings are tied to the particular meteorology of this 7-month period. How does this compare to the year-to-year and long term variability?

Longterm collection of wind radiometers may provide additional observations to study diurnal wind variability over the longer term, e.g.

- 1) Better understandings of the mechanisms that influence joint diurnal variability of ocean winds, and oceanic convection discerned by TRMM/GPM
- 2) Provide a more rigorous model assessment (e.g., can the model replicate not only speed/direction, but also diurnal variability?)
- 3) Extend coverage more globally outside of moored arrays (e.g., Global Tropical Moored Buoy Array)

TAO-TRITON Observed Surface Convergence Over Oceanic Basins

15 FEBRUARY 2008

UEYAMA AND DESER

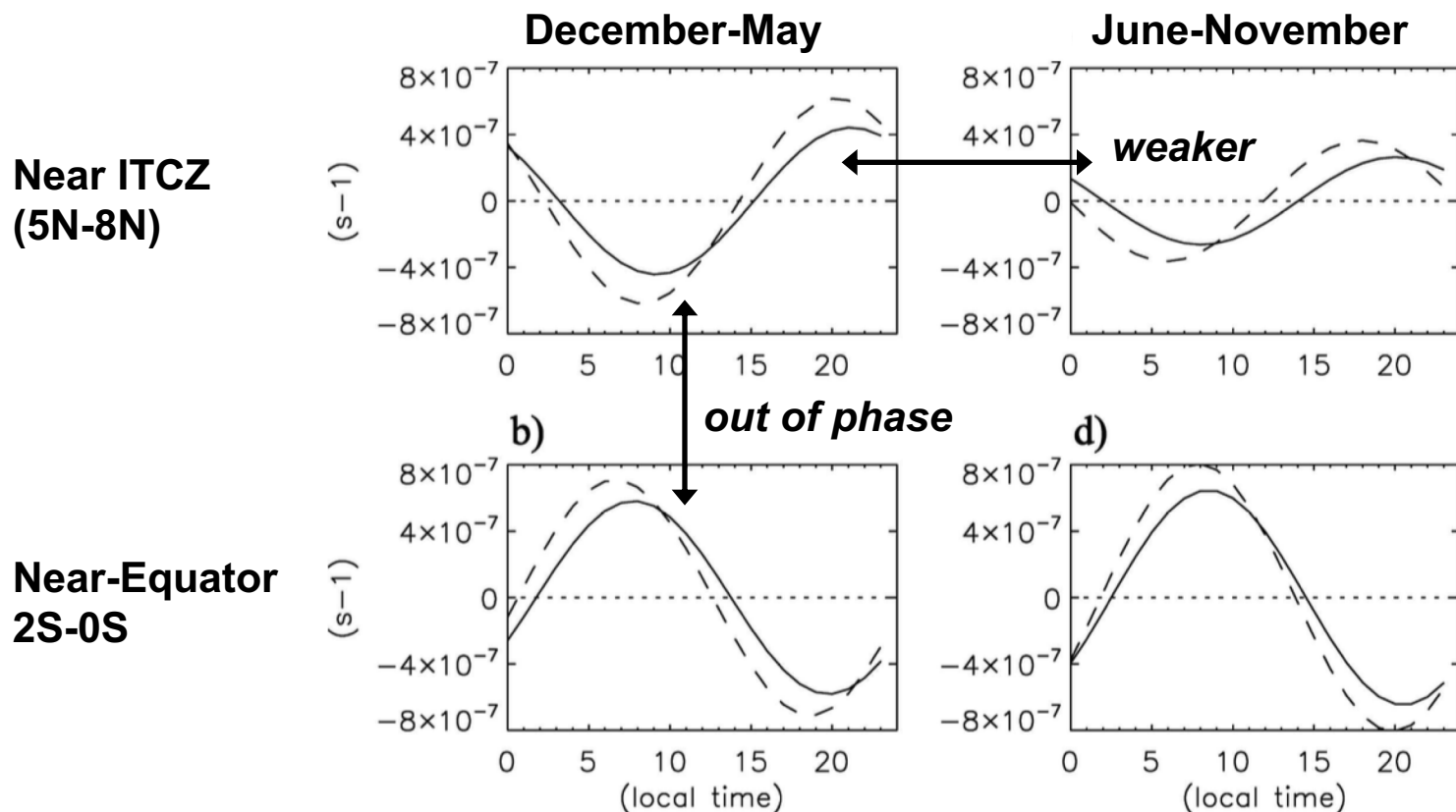
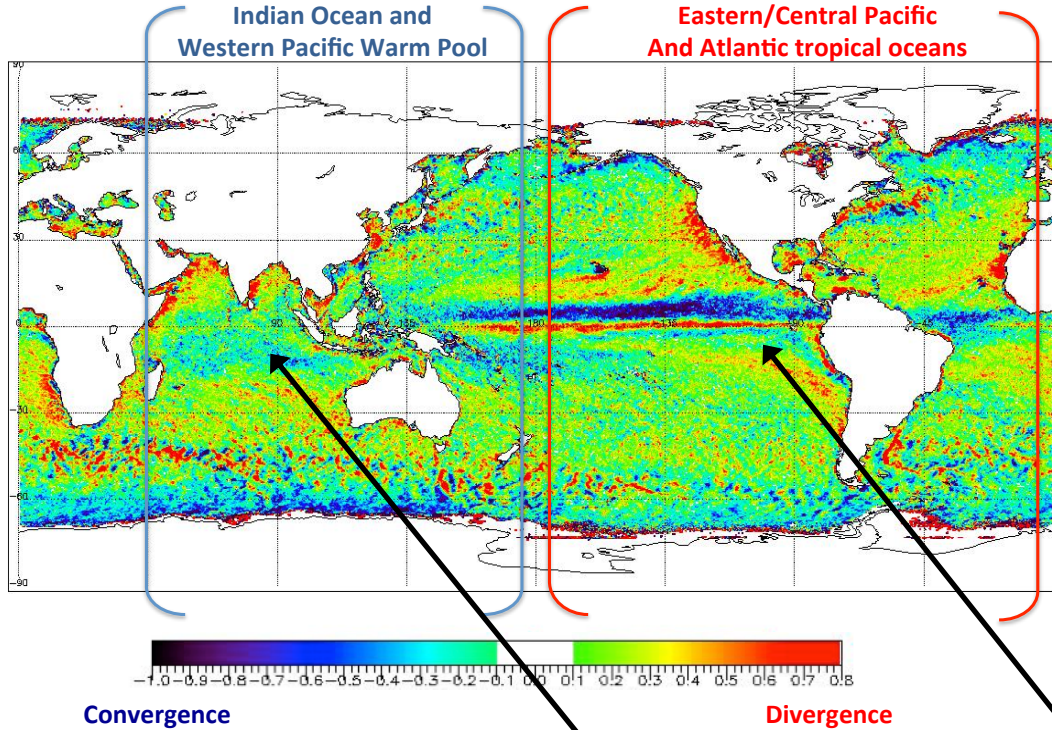


FIG. 14. (left) December–May and (right) June–November diurnal cycle (LT) of surface wind divergence (s^{-1}) averaged over all longitudes ($165^{\circ}E$ – $95^{\circ}W$; solid) and western longitudes ($165^{\circ}E$ – $155^{\circ}W$; dashed) for (a), (c) near-ITCZ (8° – $5^{\circ}N$) and (b), (d) near-equatorial (0° – $2^{\circ}S$) regions. All available wind data (including buoys with $<50\%$ data coverage, Table 1) were analyzed. The daily means at each buoy have been removed. Positive (negative) values indicate divergence (convergence) relative to the daily mean.

All Longitudes 166E-95W (solid)

Only West Pacific 165E-155W (dash)

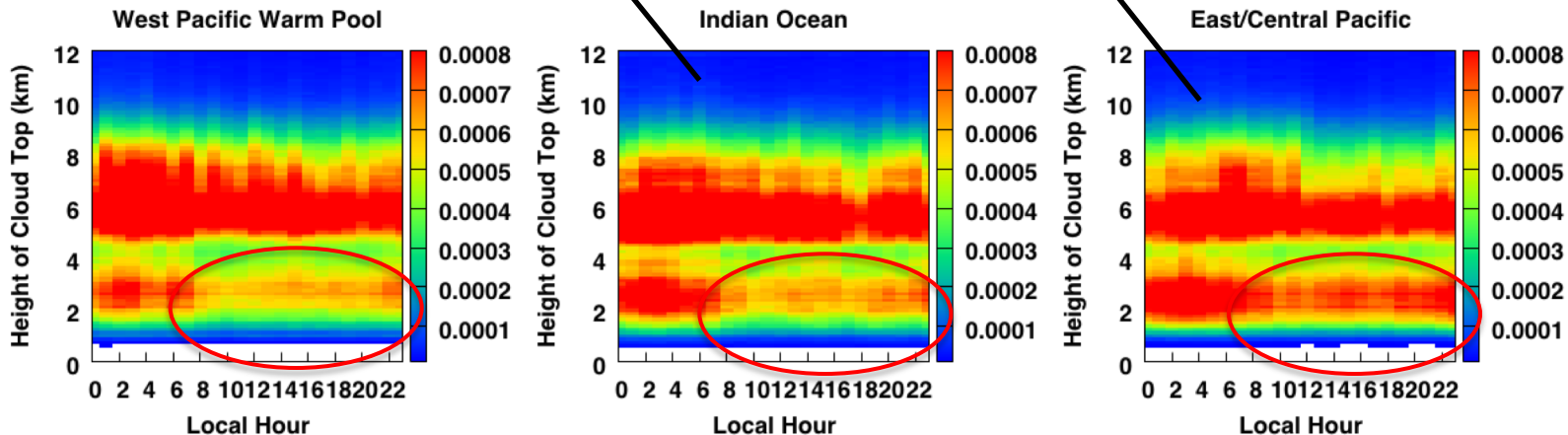
Surface Convergence and Precipitation Structure Over Oceanic Basins



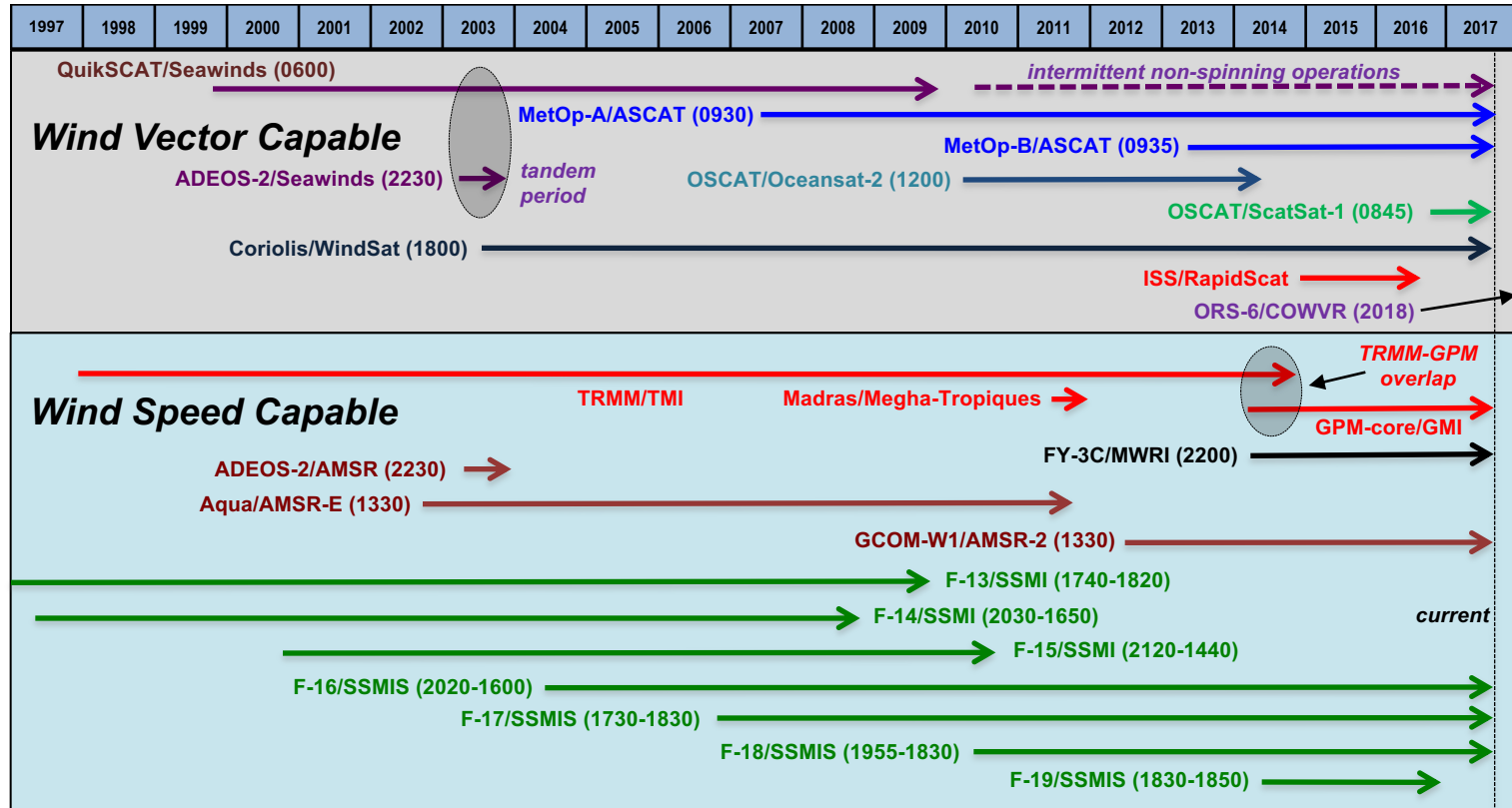
QuikSCAT (2008) data reveals stronger convergence in the East/Central Pacific relative to Indian/West Pacific

GPM DPR Radar Profile reveals a stronger late afternoon shallow precipitation mode in the East/Central Pacific, relative to Indian/West Pacific basins

DPR 20 dB Cloud Top Height (GPM 2014-2017)



Current and Near-Future Constellation of Scatterometers, Radiometers and Microwave Polarimeters



DMSF F-20 no plans to fly

GMI-2 looking for a partner, last I heard

AMSR-3 maybe....

COWVR on ORS-6 planned for 2018 (polarimeter like WindSat)

GPM-core has sufficient fuel for into the 2030s

Principle (recap from 2017 OVWST poster)

For the speed-only (w) radiometers, since the relation between w and the u and v components is non-linear, hypothetical vectors are created by varying the directions one degree at a time (e.g., for one radiometer):

$$u_{n+1} = w \cos(\theta) = a_0 + a_1 \cos(2\pi t_1 / 24) + a_2 \sin(2\pi t_1 / 24) + a_3 \cos(4\pi t_1 / 24) + a_4 \cos(4\pi t_1 / 24)$$

$$v_{n+1} = w \sin(\theta) = b_0 + b_1 \cos(2\pi t_1 / 24) + b_2 \sin(2\pi t_1 / 24) + b_3 \cos(4\pi t_1 / 24) + b_4 \cos(4\pi t_1 / 24)$$

$$E(\theta) = \min \left(\sum_{i=1}^n (u_{n+1} - u_i)^2 + (v_{n+1} - v_i)^2 \right)$$



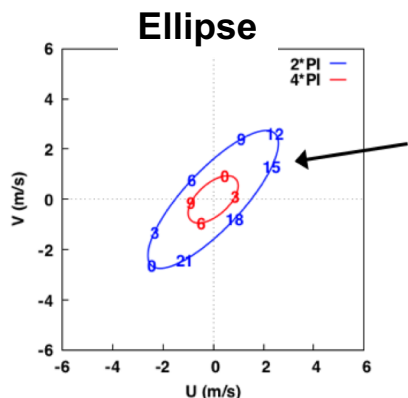
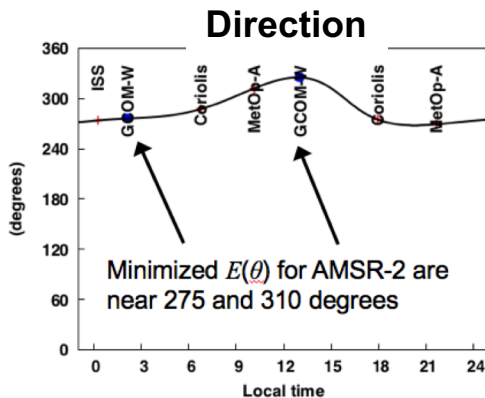
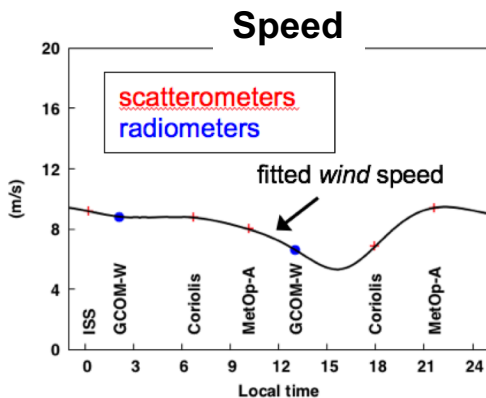
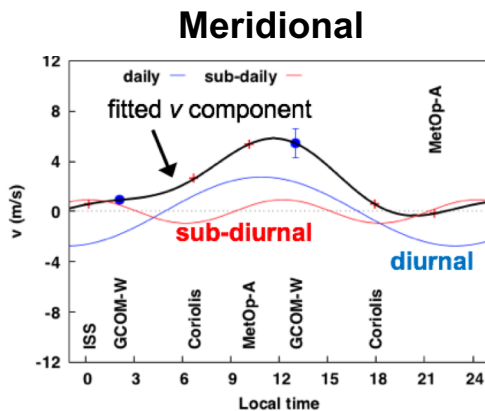
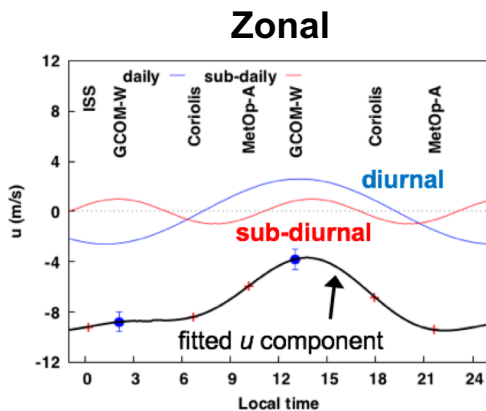
Locate the directions θ that best agree with the observed vectors.

In either the diurnal-only or semidiurnal case, these expressions can be expressed in matrix form, where D_u and D_v are diagonal matrices with the variance of the u and v observations.

$$\hat{x} = \left(A^T D_u^{-1} A \right)^{-1} A^T D_u^{-1} U$$

$$\hat{y} = \left(A^T D_v^{-1} A \right)^{-1} A^T D_v^{-1} V$$

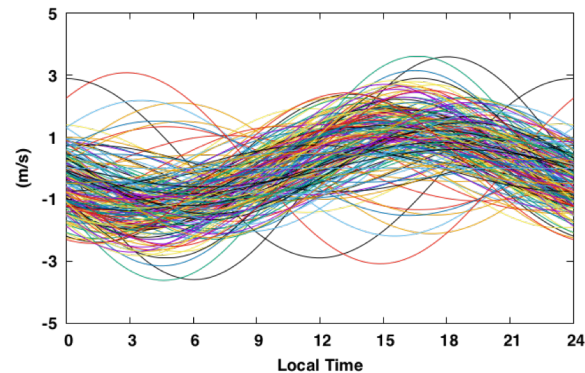
Example (16 May 2016) Offshore of Yucatan coast



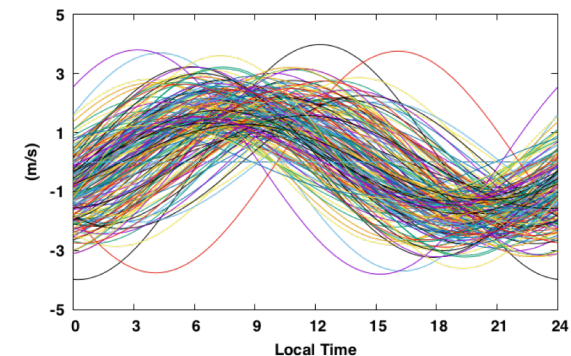
RapidScat, 2 ASCAT,
2 WindSat, 2 AMSR-2

Both the **diurnal** and **sub-diurnal** wind ellipses spin CW with magnitudes $< 3 \text{ m s}^{-1}$.

Colombia Zonal component
N= 179 20030412 - 20160201



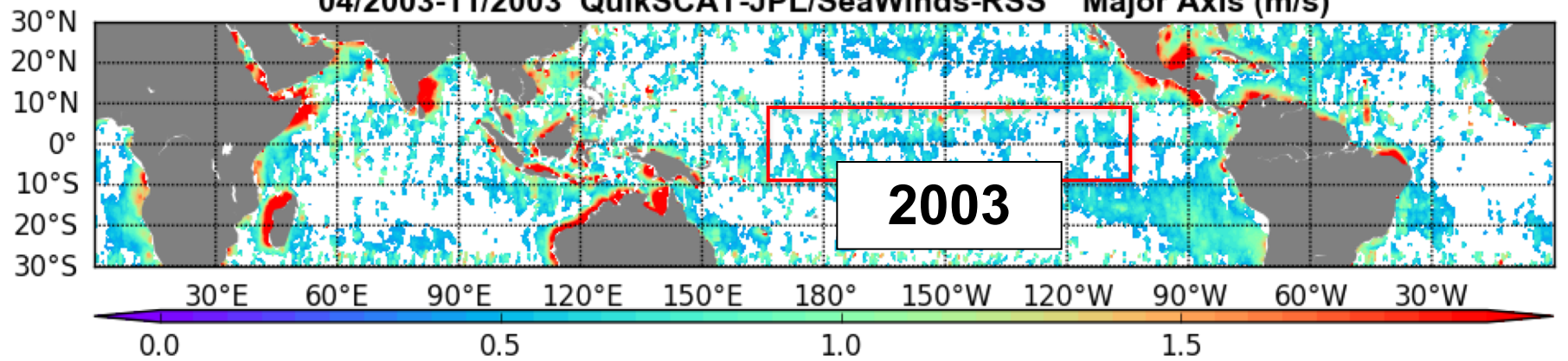
Colombia Meridional component
N= 179 20030412 - 20160201



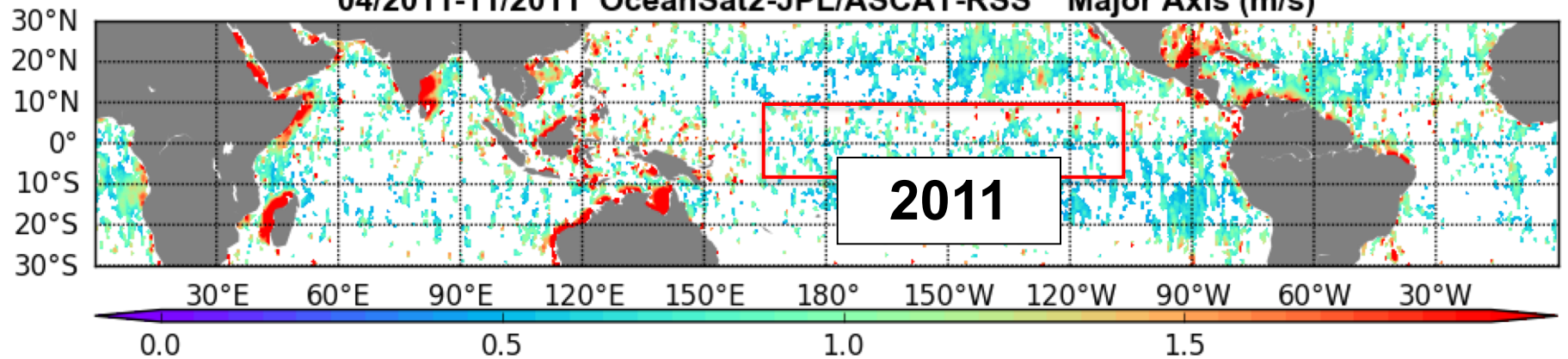
Offshore of Colombia coast

Each line is one of the days where R^2 values exceeded 0.9 during 2003-2016, all scatterometers and radiometers (SCAT+RAD)

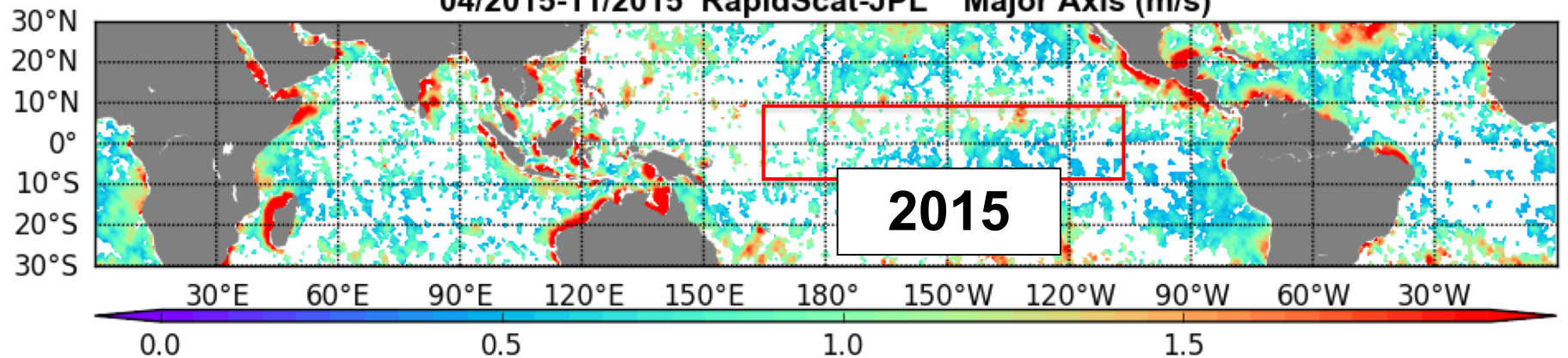
04/2003-11/2003 QuikSCAT-JPL/SeaWinds-RSS Major Axis (m/s)



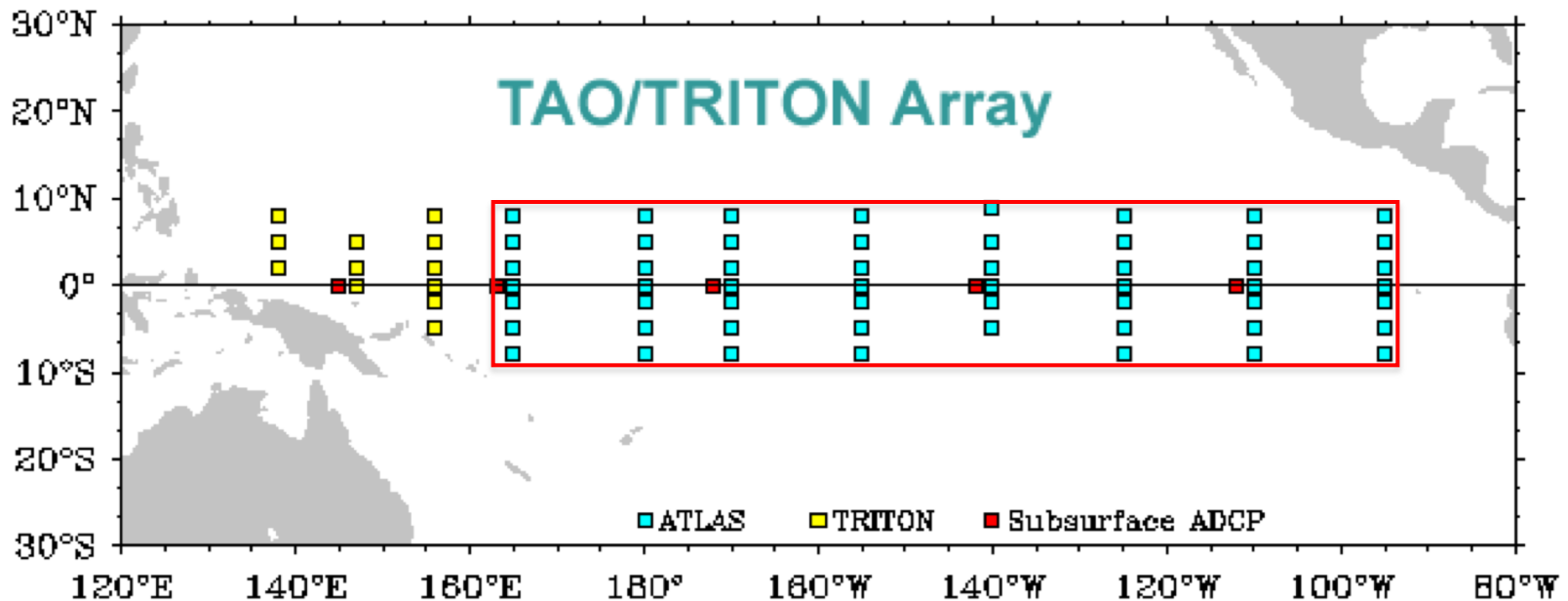
04/2011-11/2011 OceanSat2-JPL/ASCAT-RSS Major Axis (m/s)



04/2015-11/2015 RapidScat-JPL Major Axis (m/s)



Compare daily wind harmonic components estimated for all scatterometer + radiometer observations within a surrounding 1-degree box at TAO/TRITON array locations

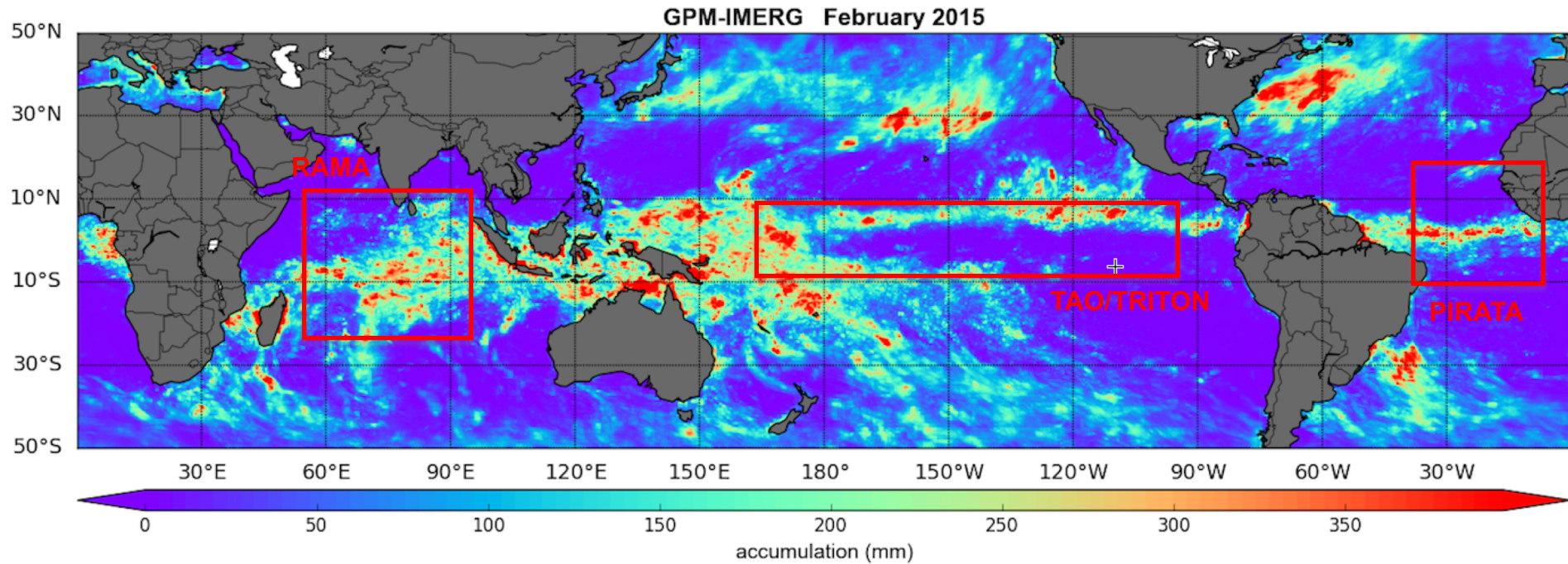


Kilpatrick et al (2017) studied the extent of the offshore propagation of the land breeze and its effect on diurnal rainfall signals in the Bay of Bengal

Previous studies (Deser & Smith 1998; Ueyema and Deser, 2007; Wood et al 2009) have suggested that far enough offshore, the tropical ocean diurnal cycle is an equatorially symmetric response to the diurnal cycle of tropical convection

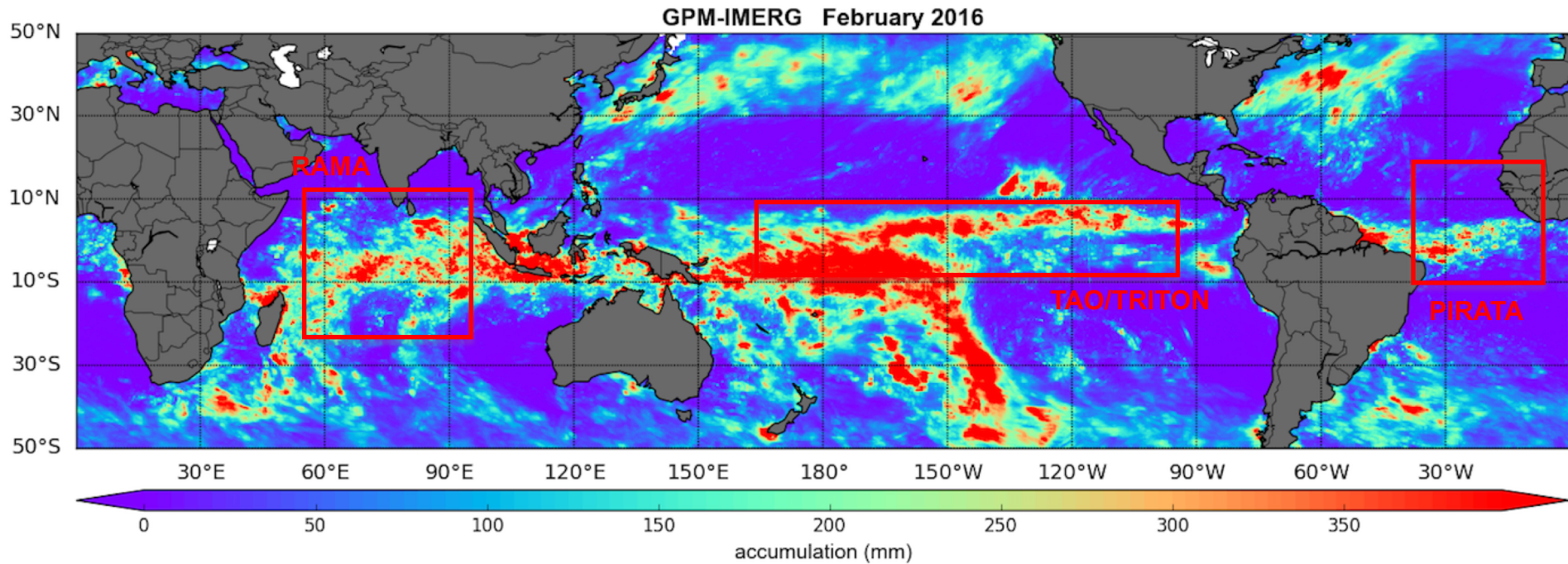
Extending the Diurnal Winds Analysis to Cover More El Niño and intraseason events

Monthly Precipitation February 2015



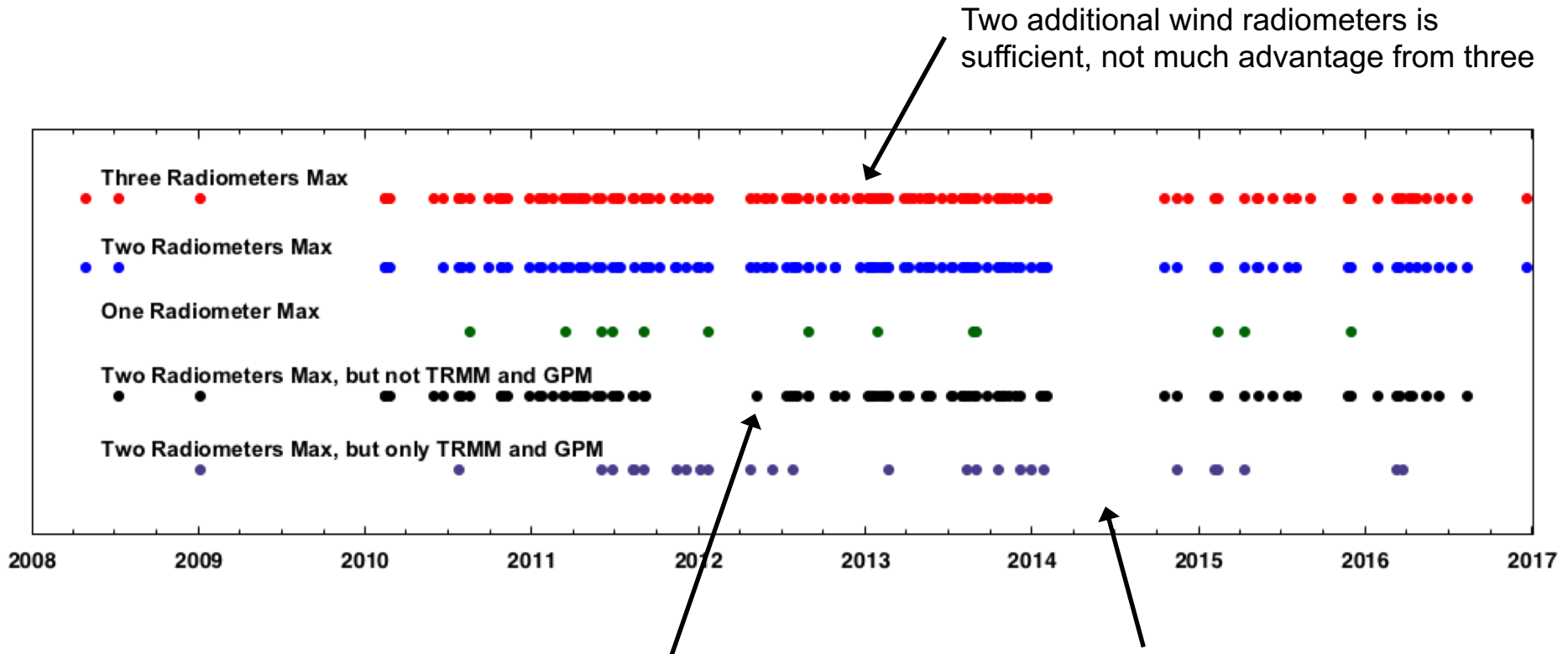
Extending the Diurnal Winds Analysis to Cover More El Nino and intraseasonal events

Monthly Precipitation February 2016



Example from a specific 1-degree region at 2S 125W

Time sequence of days where there are at least 12 u and v observations surrounding the TAO mooring located at 2S 125W, sufficient to solve equation for sub-daily variability with at least two extra degrees of freedom

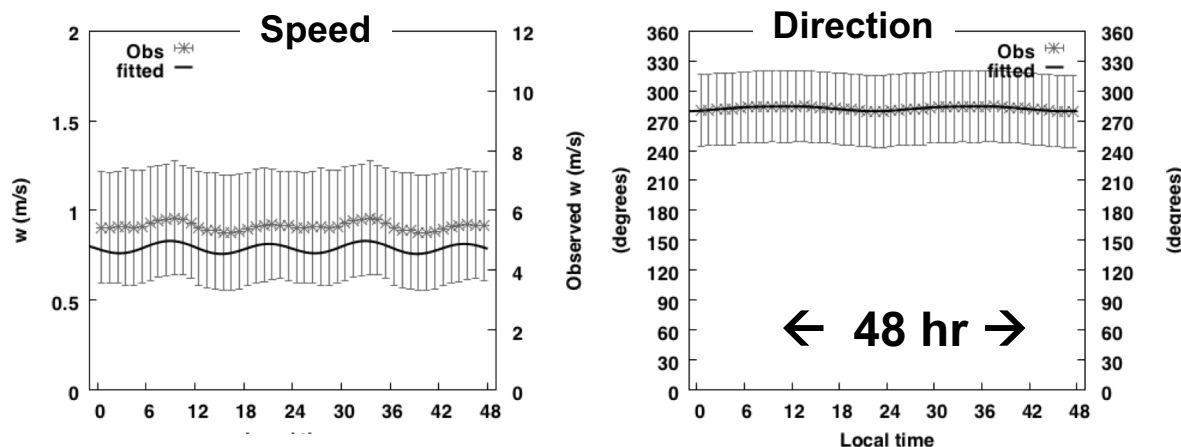
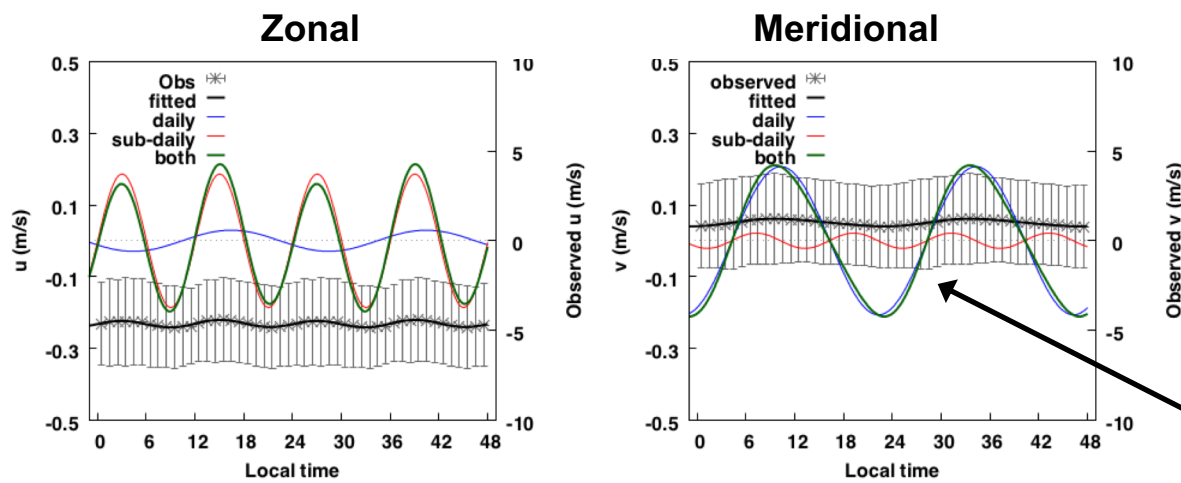


Not surprisingly, asynchronous TRMM/GPM more useful than the abundant sun-synch radiometers

Gap in 2014 occurs in the period after OceanSat-2 had ceased functioning, but RapidScat had not yet been deployed

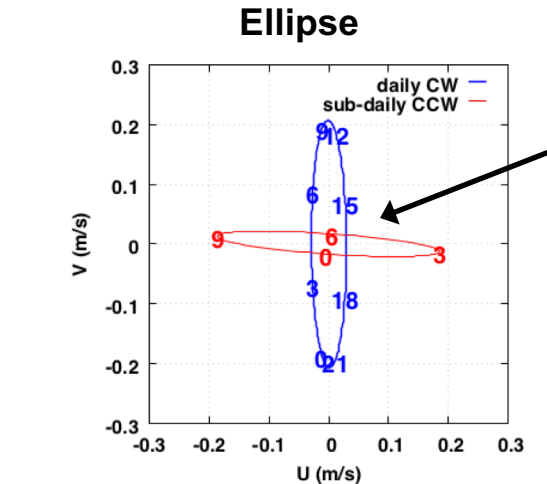
One Year (2015)
2S 155W

TAO/TRITON
(10-min data
averaged to hourly)



* observations & std dev
— overall fit

— diurnal
— semi-diurnal
— diurnal + semi-diurnal

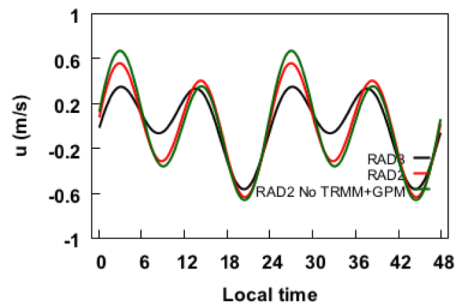


diurnal spins CW
semi-diurnal spins CCW

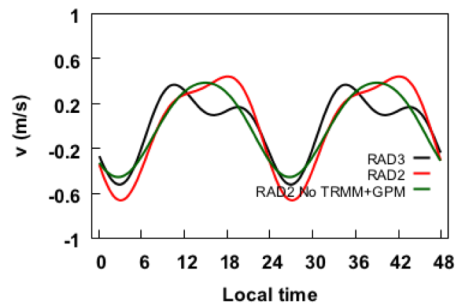
Zonal is mostly semi-diurnal, owing to the presence of the semi-diurnal tidal pressure wave prevalent in the tropics

Meridional is mostly diurnal, less understood and more variable

08N 155W SCAT+RAD



08N 155W SCAT+RAD



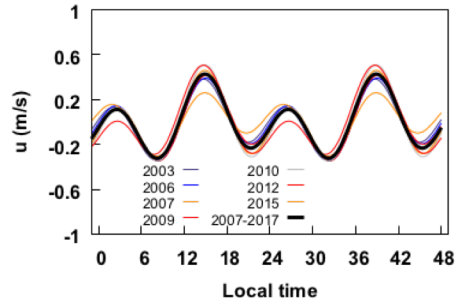
SCAT+RAD

Left: u Right: v
2 Rad **3 Rad**

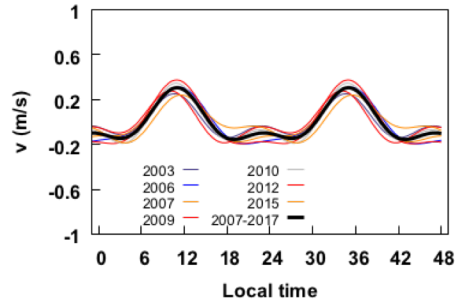
8N 155W

For data sufficiency,
SCAT+RAD
analysis extends
over 2007-2017
period

08N 155W MERRA2



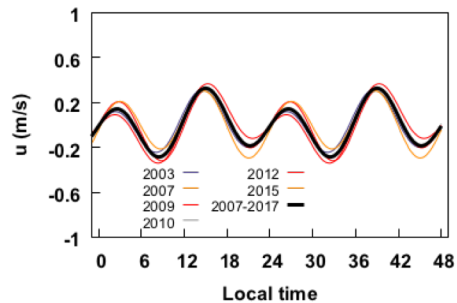
08N 155W MERRA2



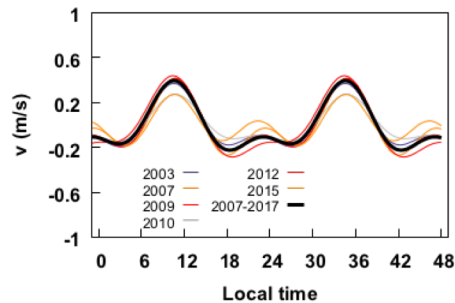
MERRA2

To show variability
throughout this
period, for the
models and
moorings each line
color represents
data from one year
(all 2007-2017 in
solid black)

08N 155W ERA-I

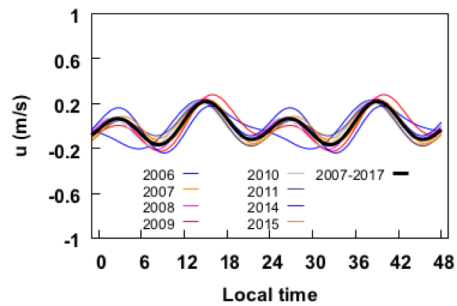


08N 155W ERA-I

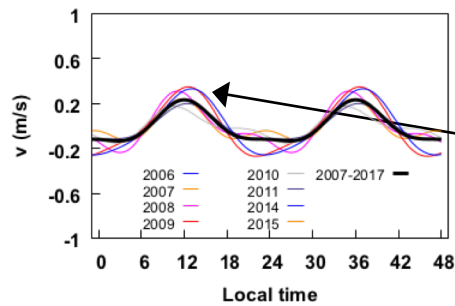


ERA-I

08N 155W TAO



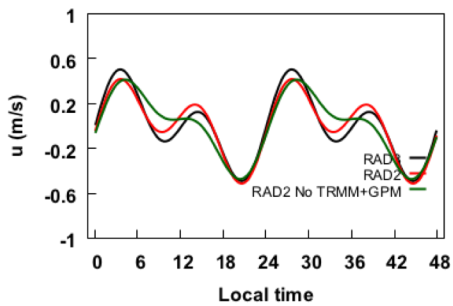
08N 155W TAO



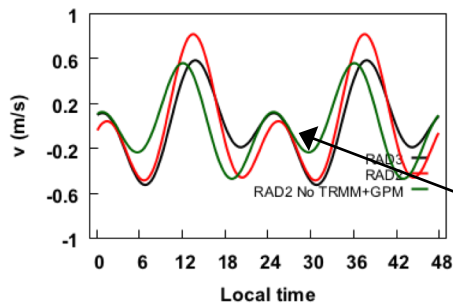
TAO-TRITON

Peak in semi-diurnal v
near 9Z, in accord with
DS and UD

05N 155W SCAT+RAD



05N 155W SCAT+RAD



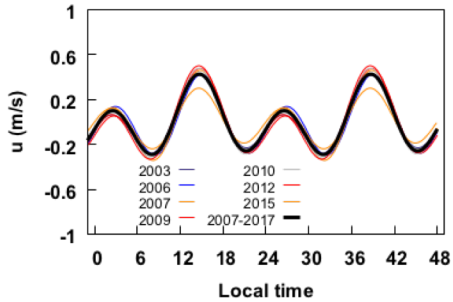
SCAT+RAD
 Left: u Right: v
 semi-diurnal component

5N 155W

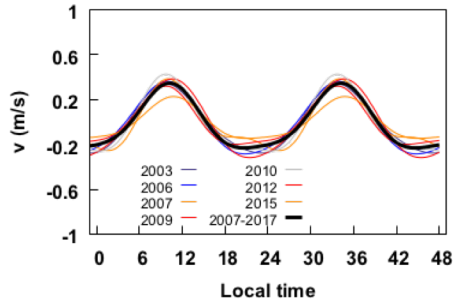
For data sufficiency, SCAT+RAD analysis extends over 2007-2017 period

To show variability throughout this period, for the models and moorings each line color represents data from one year (all 2007-2017 in solid black)

05N 155W MERRA2

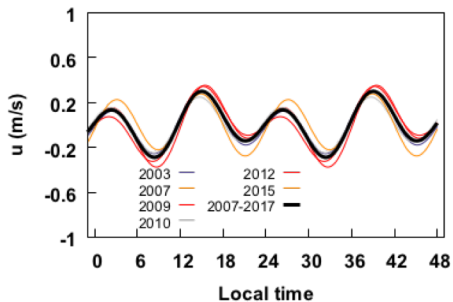


05N 155W MERRA2

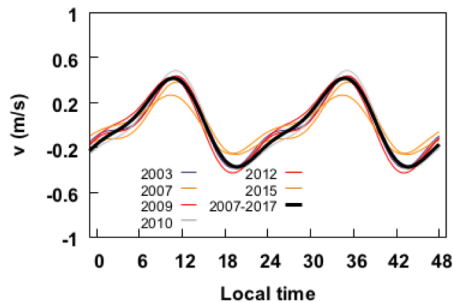


MERRA2

05N 155W ERA-I

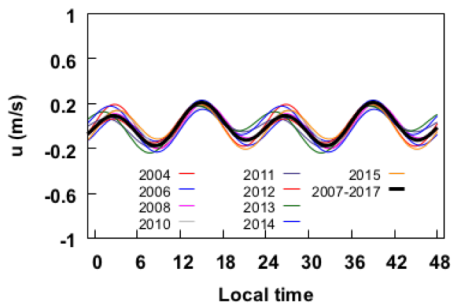


05N 155W ERA-I

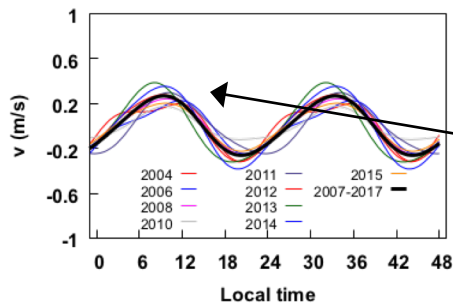


ERA-I

05N 155W TAO



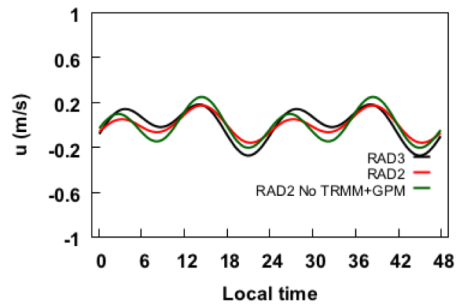
05N 155W TAO



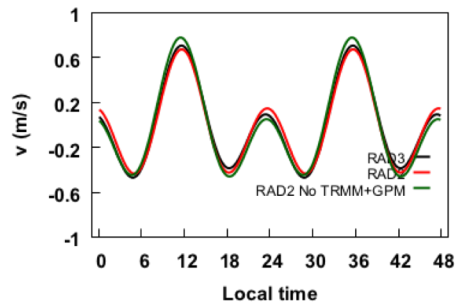
TAO-TRITON

Peak in semi-diurnal v near 9Z, in accord with DS and UD

02N 155W SCAT+RAD



02N 155W SCAT+RAD



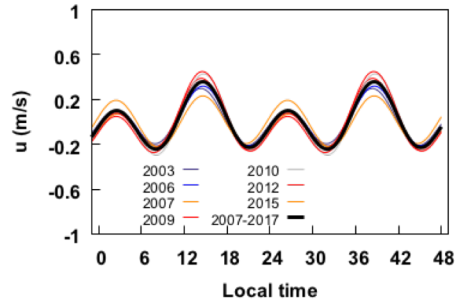
SCAT+RAD
Left: u Right: v

2N 155W

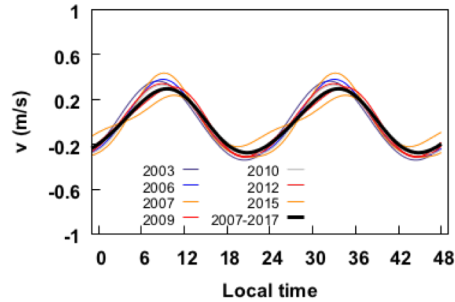
For data sufficiency,
SCAT+RAD
analysis extends
over 2007-2017
period

To show variability
throughout this
period, for the
models and
moorings each line
color represents
data from one year
(all 2007-2017 in
solid black)

02N 155W MERRA2

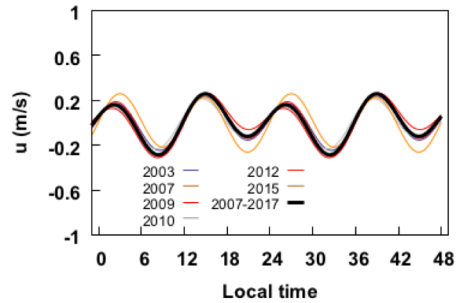


02N 155W MERRA2

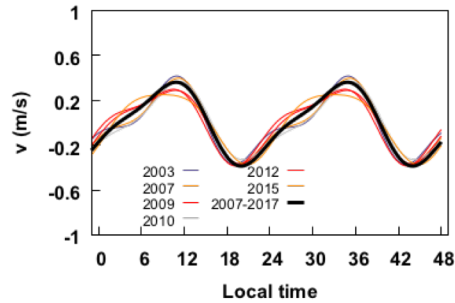


MERRA2

02N 155W ERA-I

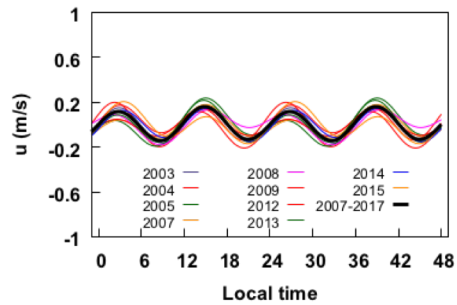


02N 155W ERA-I

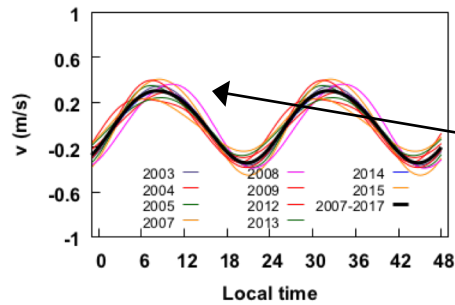


ERA-I

02N 155W TAO



02N 155W TAO



TAO-TRITON

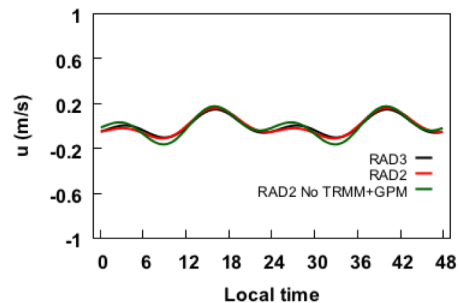
Peak in semi-diurnal v
near 9Z, in accord with
DS and UD

2S 155W

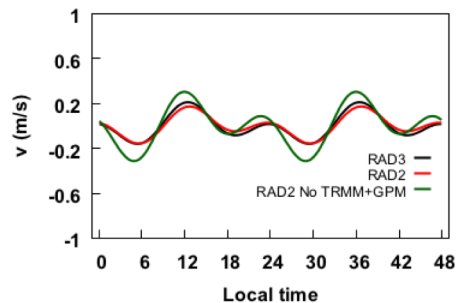
For data sufficiency,
SCAT+RAD
analysis extends
over 2007-2017
period

To show variability
throughout this
period, for the
models and
moorings each line
color represents
data from one year
(all 2007-2017 in
solid black)

02S 155W SCAT+RAD



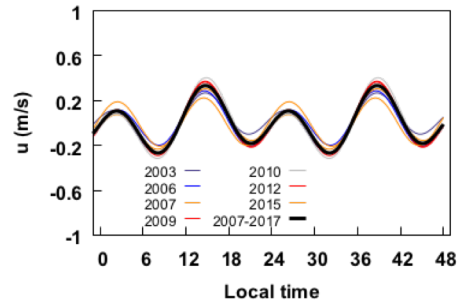
02S 155W SCAT+RAD



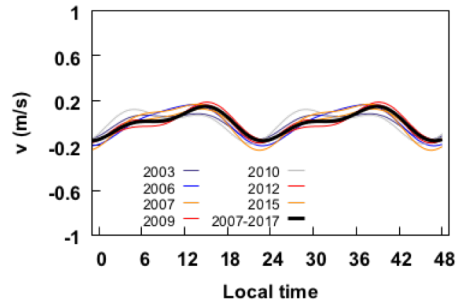
SCAT+RAD

Left: u Right: v

02S 155W MERRA2

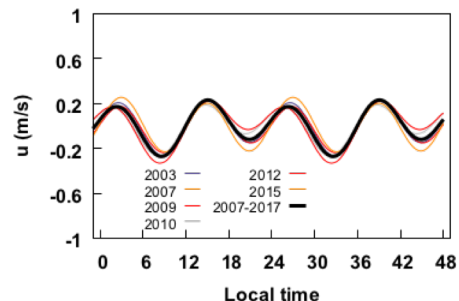


02S 155W MERRA2

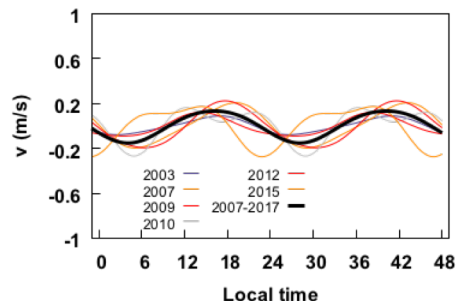


MERRA2

02S 155W ERA-I

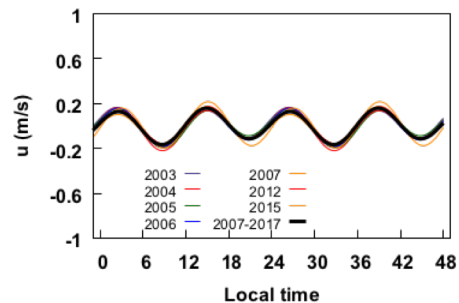


02S 155W ERA-I

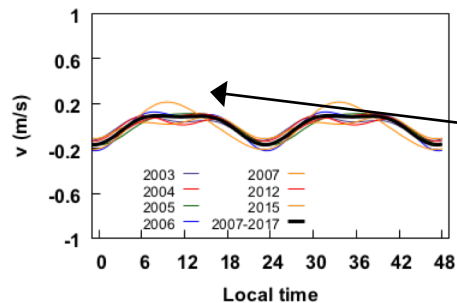


ERA-I

02S 155W TAO



02S 155W TAO



TAO-TRITON

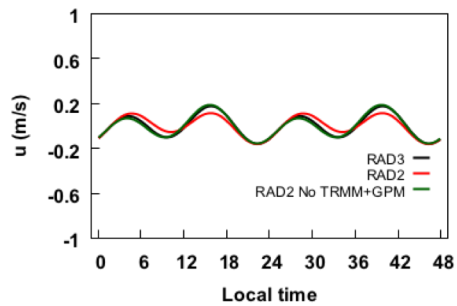
Peak in semi-diurnal v
begins to shift to late
afternoon

5S 155W

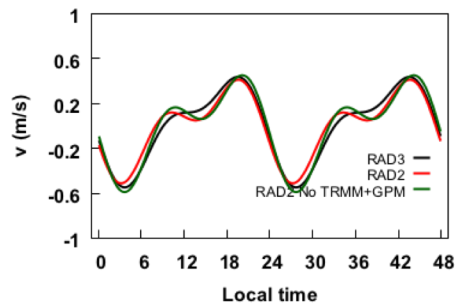
For data sufficiency, SCAT+RAD analysis extends over 2007-2017 period

To show variability throughout this period, for the models and moorings each line color represents data from one year (all 2007-2017 in solid black)

05S 155W SCAT+RAD

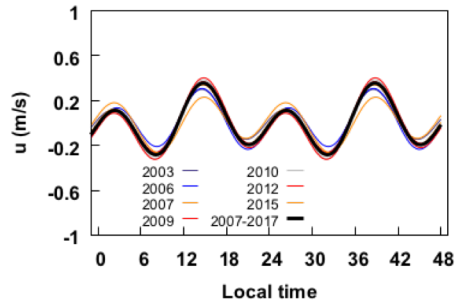


05S 155W SCAT+RAD

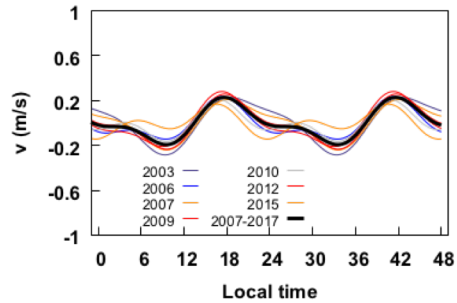


SCAT+RAD
Left: u Right: v

05S 155W MERRA2

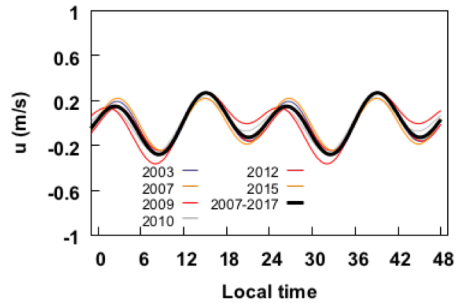


05S 155W MERRA2

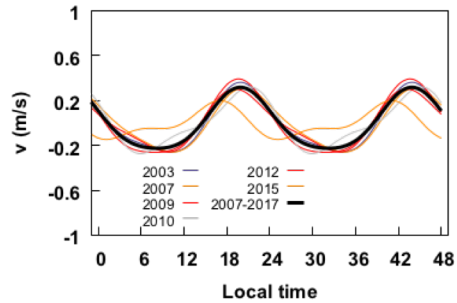


MERRA2

05S 155W ERA-I

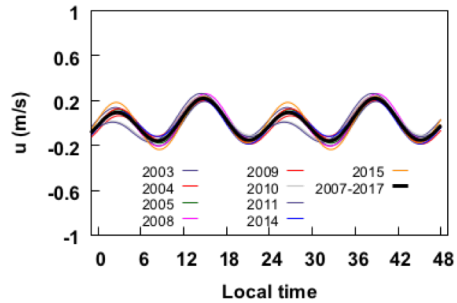


05S 155W ERA-I

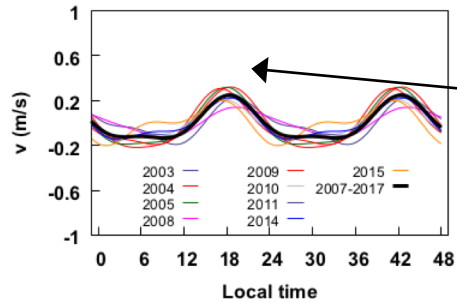


ERA-I

05S 155W TAO



05S 155W TAO



TAO-TRITON

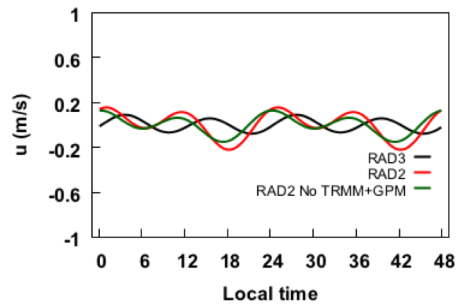
Peak in semi-diurnal v near 18-19Z

8S 155W

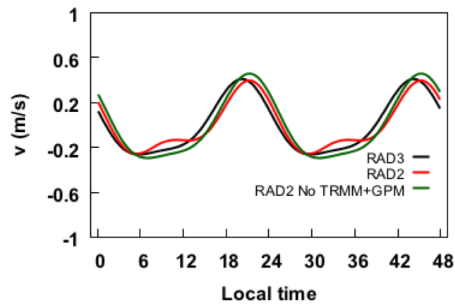
For data sufficiency, SCAT+RAD analysis extends over 2007-2017 period

To show variability throughout this period, for the models and moorings each line color represents data from one year (all 2007-2017 in solid black)

08S 155W SCAT+RAD

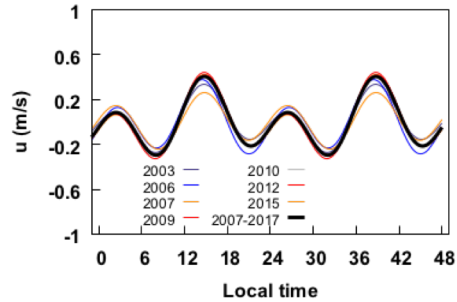


08S 155W SCAT+RAD

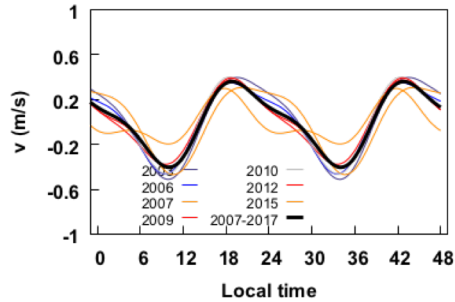


SCAT+RAD
Left: u Right: v

08S 155W MERRA2

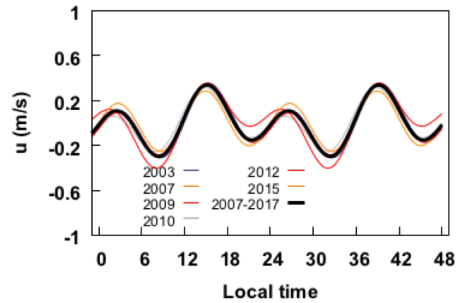


08S 155W MERRA2

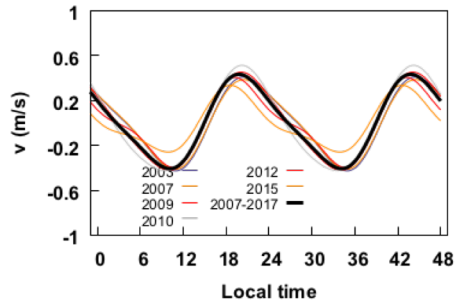


MERRA2

08S 155W ERA-I

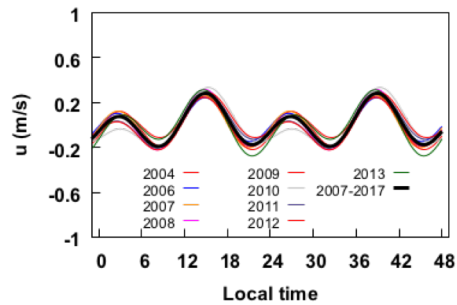


08S 155W ERA-I

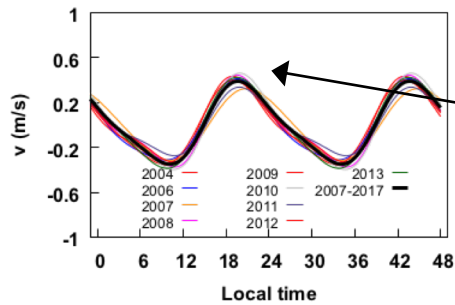


ERA-I

08S 155W TAO



08S 155W TAO



TAO-TRITON

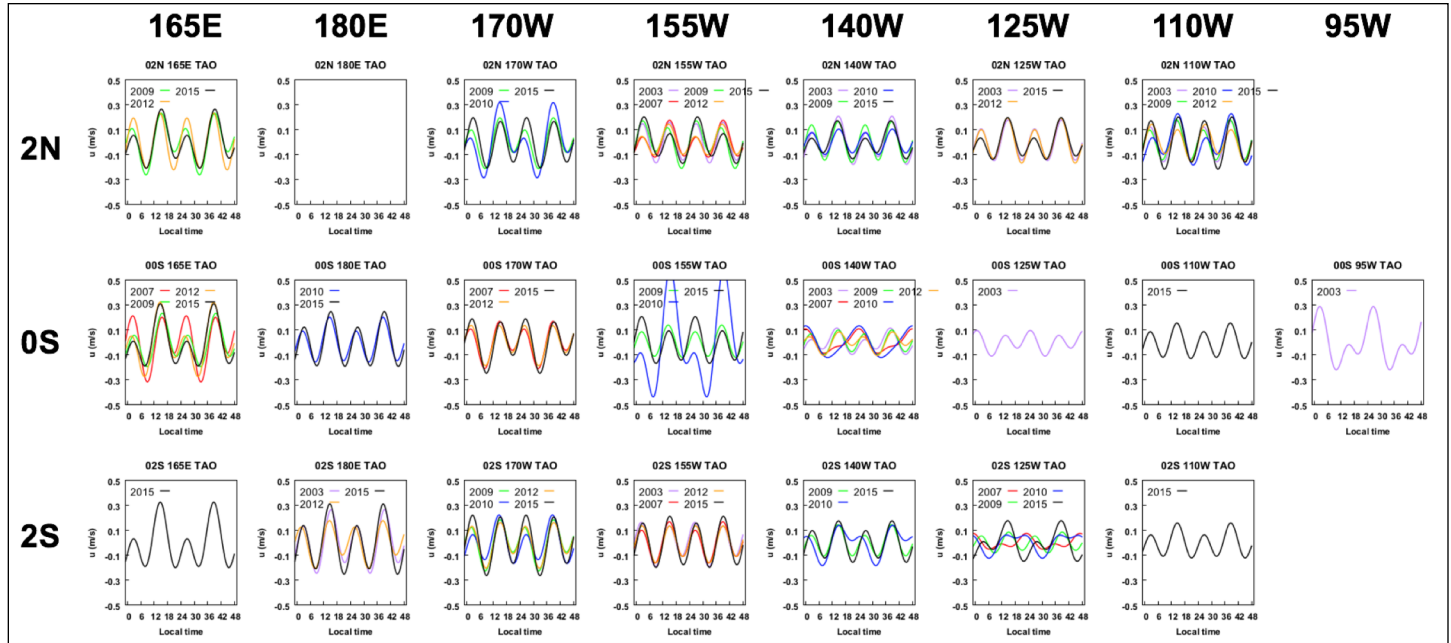
Peak in semi-diurnal v near 19Z, in accord with DS and UD

TAO-TRITON

individual years

Each panel: x-axis extends 0-48 hr local. y-axis extends ± 2 m/s.

Zonal \rightarrow

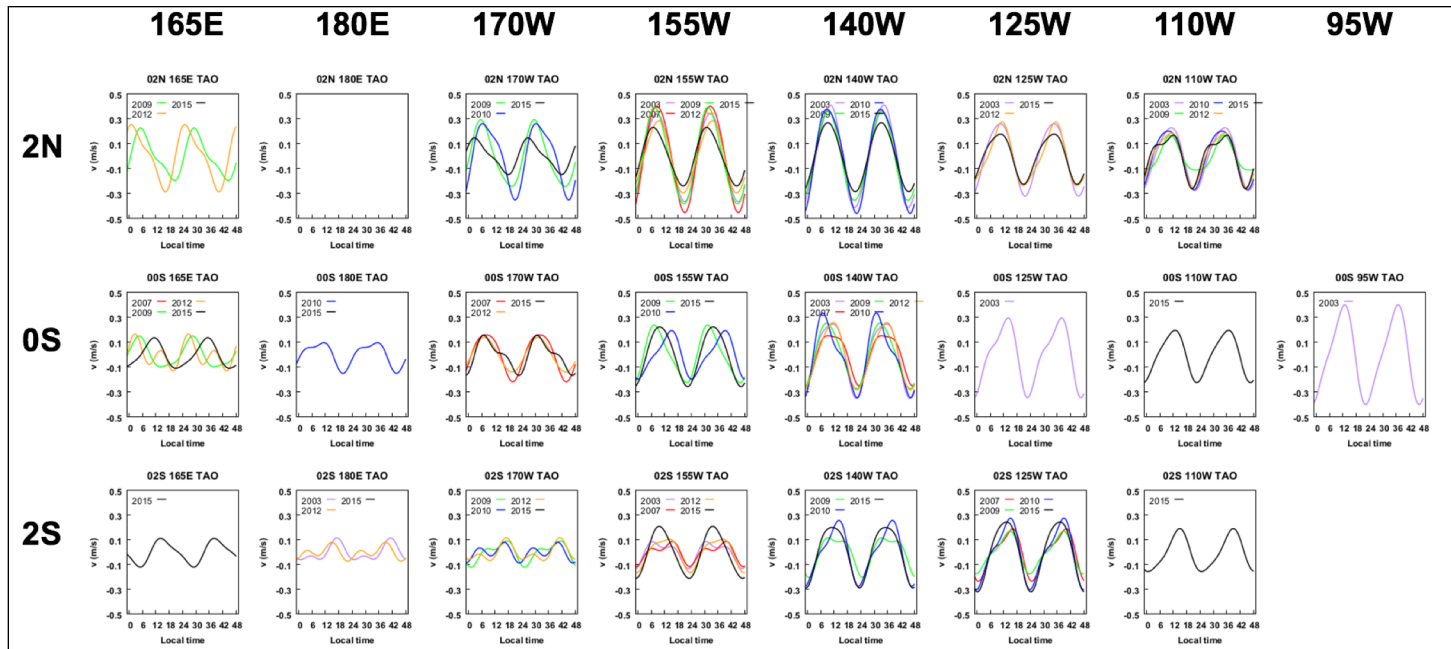


Each panel:

x-axis
extends
0-48 hr local

y-axis
extends
 ± 2 m/s

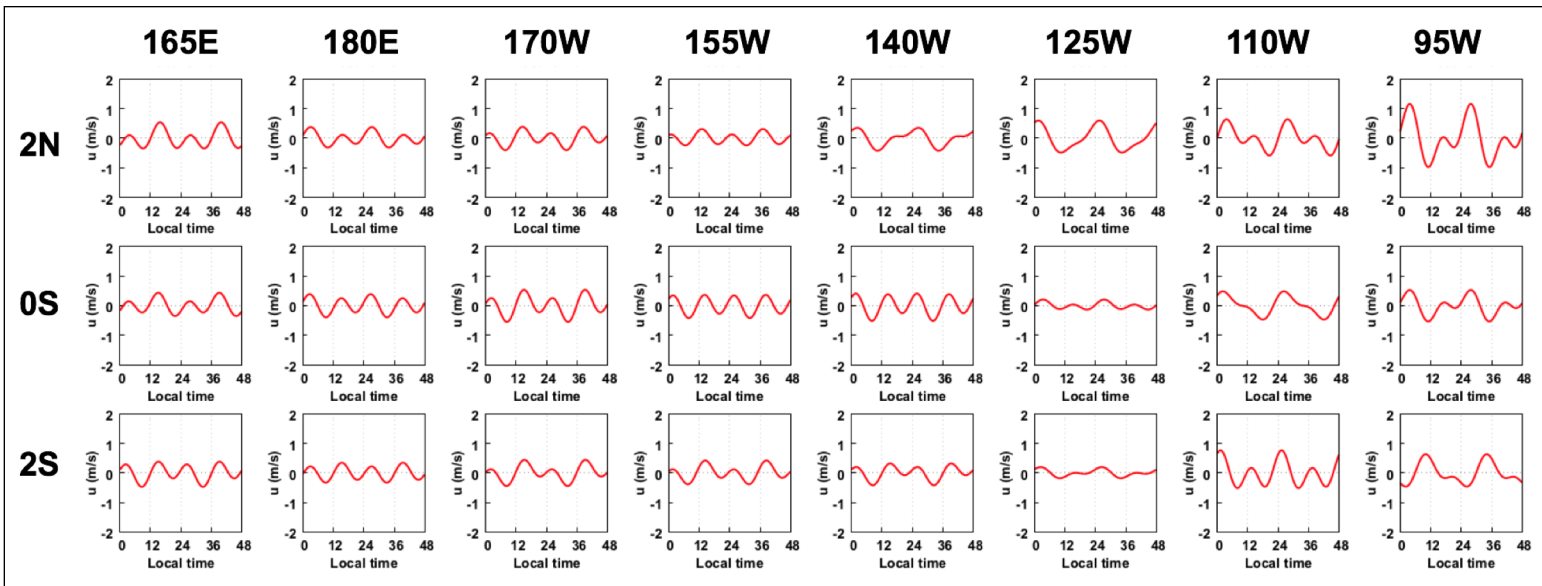
Meridional \rightarrow



SCAT+RAD (2007-2017)

Each panel: x-axis extends 0-48 hr local. y-axis extends ± 2 m/s.

Zonal \rightarrow

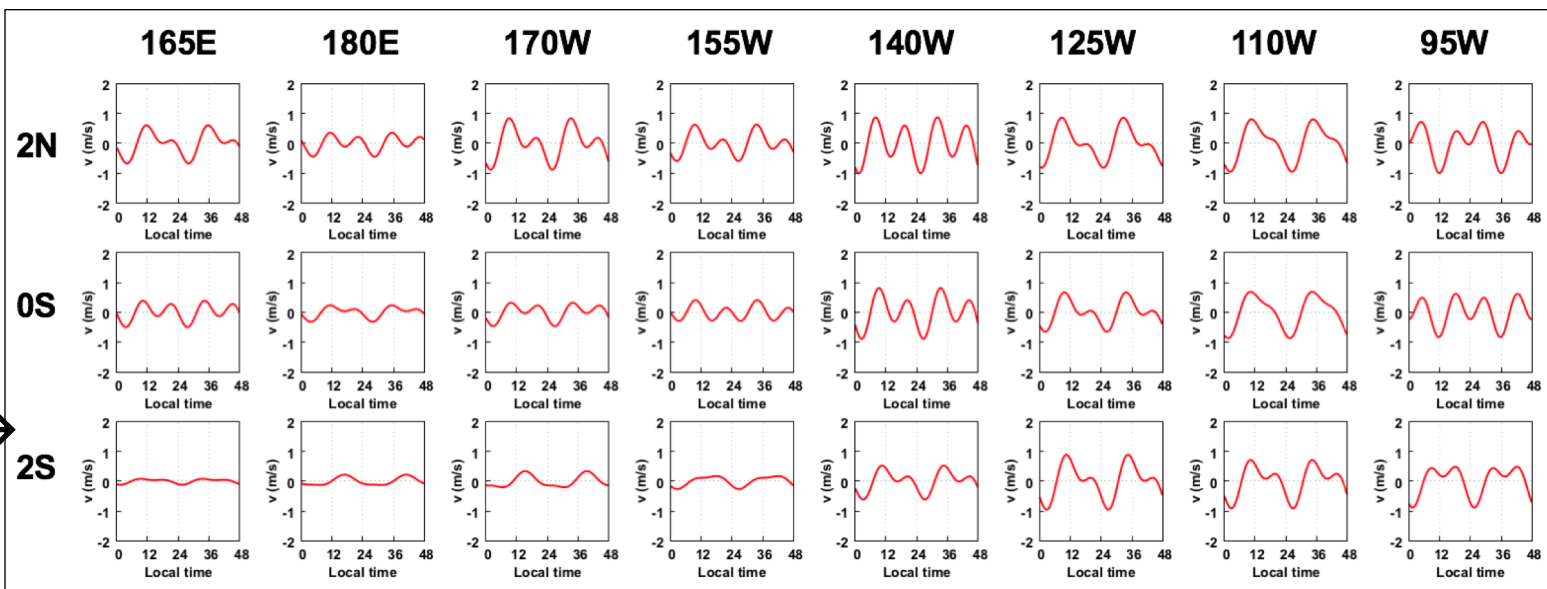


Each panel:

x-axis
extends
0-48 hr local

y-axis
extends
 ± 2 m/s

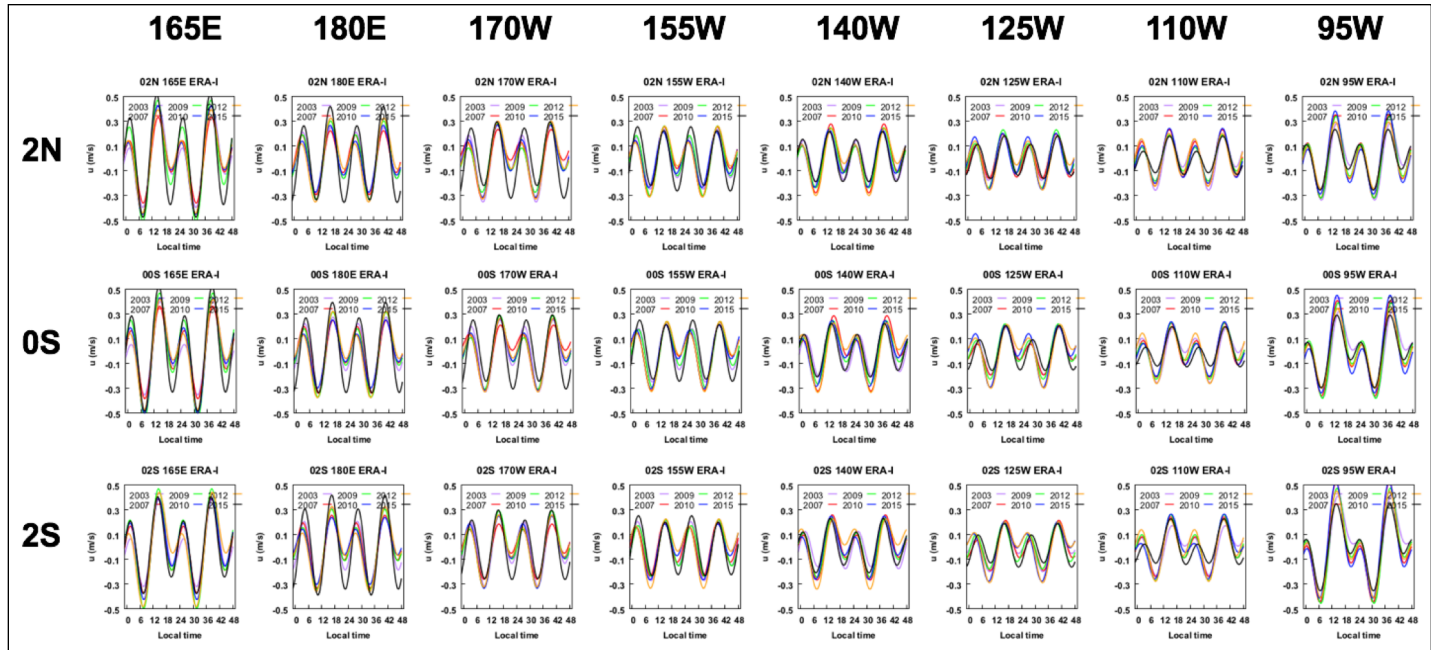
Meridional \rightarrow



ERA-I individual years

Each panel: x-axis extends 0-48 hr local. y-axis extends ± 2 m/s.

Zonal \rightarrow

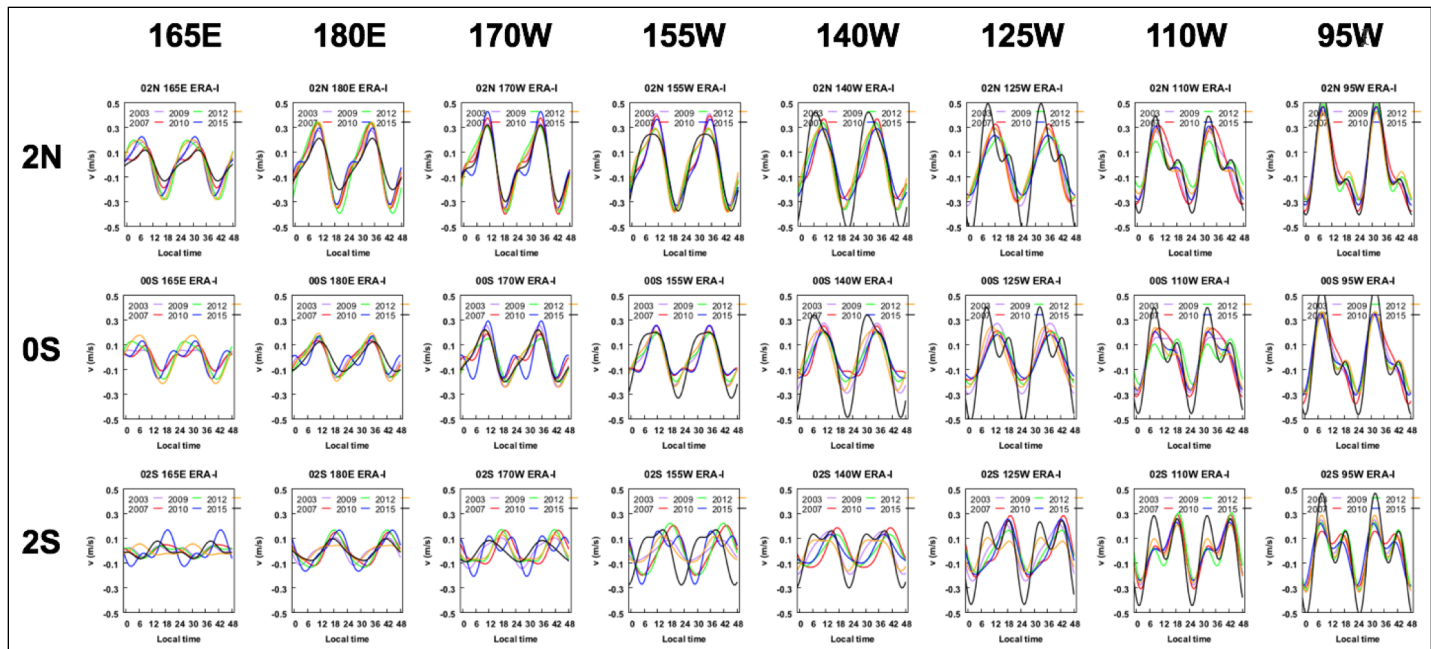


Each panel:

x-axis
extends
0-48 hr local

y-axis
extends
 ± 2 m/s

Meridional \rightarrow



Summary

At some locations, the 10-year (2007-2017) scat+rad daily wind mode record captures the semi-diurnal zonal wind noted by the tropical moorings, which generally well-represented by the models

Less so for the meridional daily wind component, where year to year differences between models themselves and scat+rad appear more noticeable

Sampling is nonuniform and (non-physical) semi-diurnal components sometimes appear owing to biases between closely-spaced wind observations

Suggests a broader look at between the ITCZ ocean surface daily wind modes, regions of strong/weak convergence, and year-to-year differences in the diurnal convective cloud structure from TRMM/GPM

More thought put into proper matching framework amongst models, satellite winds, moorings before drawing further conclusions